AD-A043 272 BALLISTIC RESEARCH LABS ABERDEEN PROVING GROUND MD F/G 20/8
PHOTODISSOCIATION OF NO(+)(NO) AND NO(+)(H2O).(U)
JUL 77 J A VANDERHOFF

UNCLASSIFIED BRL-1994 NL

| OF |
AD
A043272

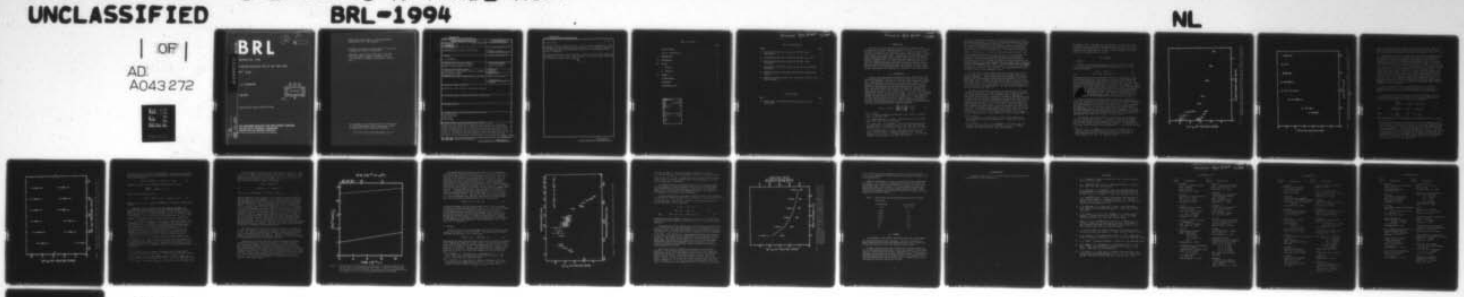

END
DATE
FILMED
9-77
DDC

BRL R 1994

BRL

(12)

AD

REPORT NO. 1994

PHOTODISSOCIATION OF $NO^+(NO)$ AND $NO^+(H_2O)$

J. A. Vanderhoff

July 1977

USA ARMAMENT RESEARCH AND DEVELOPMENT COMMAND
USA BALLISTIC RESEARCH LABORATORY
ABERDEEN PROVING GROUND, MARYLAND

Destroy this report when it is no longer needed.
Do not return it to the originator.

Secondary distribution of this report by originating or sponsoring activity is prohibited.

Additional copies of this report may be obtained from the National Technical Information Service, U.S. Department of Commerce, Springfield, Virginia 22151.

The findings in this report are not to be construed as an official Department of the Army position, unless so designated by other authorized documents.

The use of trade names or manufacturers' names in this report does not constitute indorsement of any commercial product.

UNCLASSIFIED

SECURITY CLASSIFICATION OF THIS PAGE *(When Data Entered)*

REPORT DOCUMENTATION PAGE		READ INSTRUCTIONS BEFORE COMPLETING FORM
1. REPORT NUMBER BRL Report No. 1994	2. GOVT ACCESSION NO.	3. RECIPIENT'S CATALOG NUMBER
4. TITLE *(and Subtitle)* PHOTODISSOCIATION OF $NO^{+}_{2}(NO)$ AND $NO^{+}(H_2O)$		5. TYPE OF REPORT & PERIOD COVERED Final 6. PERFORMING ORG. REPORT NUMBER
7. AUTHOR(s) J. A. VANDERHOFF		8. CONTRACT OR GRANT NUMBER(s)
9. PERFORMING ORGANIZATION NAME AND ADDRESS US Army Ballistic Research Laboratory Aberdeen Proving Ground, MD 21005		10. PROGRAM ELEMENT, PROJECT, TASK AREA & WORK UNIT NUMBERS RDT&E 1L161102B53A
11. CONTROLLING OFFICE NAME AND ADDRESS US Army Materiel Development & Readiness Command 5001 Eisenhower Avenue Alexandria, VA 22333		12. REPORT DATE JULY 1977 13. NUMBER OF PAGES 28
14. MONITORING AGENCY NAME & ADDRESS*(if different from Controlling Office)* 12 23p.		15. SECURITY CLASS. *(of this report)* Unclassified 15a. DECLASSIFICATION/DOWNGRADING SCHEDULE

16. DISTRIBUTION STATEMENT *(of this Report)*

Approved for public release; distribution unlimited.

17. DISTRIBUTION STATEMENT *(of the abstract entered in Block 20, if different from Report)*

18. SUPPLEMENTARY NOTES

19. KEY WORDS *(Continue on reverse side if necessary and identify by block number)*

Photodissociation
Nitric Oxide Ions
Cluster Ions
Cross Sections

20. ABSTRACT *(Continue on reverse side if necessary and identify by block number)* (eal)

A drift tube mass spectrometer coupled with ion laser and ion laser pumped tunable dye laser photon sources has been used to measure the thermal energy (300K) photodissociation cross sections for two positive ion clusters, nitric oxide clustered with the nitric oxide ion and water clustered with the nitric oxide ion. Measurements were made spanning a photon wavelength range from 799 to 350 nm. The absolute photodissociation cross sections for nitric oxide clustered with the nitric oxide ion were found to vary smoothly with photon → next page (Contd)

DD FORM 1 JAN 73 1473 EDITION OF 1 NOV 65 IS OBSOLETE

050 750

UNCLASSIFIED

SECURITY CLASSIFICATION OF THIS PAGE *(When Data Entered)*

Item 20, Contd.

wavelength attaining a maximum value of 2 x 10(-17) square centimeters at ~ 650 nm decreasing at both longer and shorter wavelengths. In addition, coupling of clustering reactions into the photodissociation cross section appeared under a variety of conditions.

Photodissociation cross sections for water clustering with the nitric oxide ion were found to be small or zero. Upper limits of ~ 1 x 10(-19) square centimeters were obtained for these cross sections.

TABLE OF CONTENTS

LIST OF ILLUSTRATIONS

LIST OF TABLES

I. INTRODUCTION

Positive ion cluster reactions in the daytime D-region of the atmosphere fall into two dominant sequences;[1] one with O_2^+ as a precursor ion, the other with NO^+ as the precursor ion. Recently, weakly bound cluster ions formed from O_2^+ have been found to photodissociate[2,3] readily in the presence of visible light. Reported here are photodissociation cross section measurements for two weakly bound clusters, $NO^+(NO)$ and $NO^+(H_2O)$ formed from NO^+. For some cases these measured cross sections exhibit a dependence on photon flux, pressure, drift distance, and E/N. Two simple mechanisms which couple clustering reactions into the photodissociation measurement technique are employed to explain qualitatively this cross section dependence, and arguments are made supporting the acceptance of the reported cross sections as the actual values.

II. EXPERIMENTAL

Details of the experimental apparatus and data analysis have been described elsewhere[2-4] and thus only a brief summary will be presented here. The experiment consists of a drift tube mass spectrometer coupled with a continuous duty ion laser or dye laser photon sources. Either positive or negative ions can be extracted from the source region in which gases are bombarded by electrons produced from a hot filament. These ions drift toward a sampling aperture under the influence of a weak, uniform electric field. During this drift the ions make many thermalizing collisions with the neutral gas. Just prior to the sampling aperture the ions are intersected by a chopped laser beam. After passing through the aperture the ions are accelerated to a mass spectrometer which is tuned to transmit ions of a specified mass. Transmitted ions are detected and gated to one of two counters depending on chopper position. The following equation is used to extract a photodissociation cross section from experimentally measured parameters,

$$\sigma_{A^+}(\lambda_1) = \sigma_{O^-}(\lambda_1) \frac{\ell n\left[N_o/N(\lambda_1)\right]_{A^+}}{\ell n\left[N_o/N(\lambda_1)\right]_{O^-}} \frac{P\, v_{A^+}}{v_{O^-}} \quad . \qquad (1)$$

---

[1] E. E. Ferguson, "D-Region Ion Chemistry," Rev. Geophys. and Space Phys. 9, 997-1007 (1971).

[2] J. A. Vanderhoff and R. A. Beyer, "Photodissociation of $O_2^+(H_2O)$," Chem. Phys. Lett. 38, 532-536 (1976).

[3] R. A. Beyer and J. A. Vanderhoff, "Cross Section Measurements for Photodetachment or Photodissociation of Ions Produced in Gaseous Mixtures of O_2, CO_2, and H_2O," J. Chem. Phys. 65, 2313-2321 (1976).

[4] J. A. Vanderhoff and R. A. Beyer, "Experimental Photodissociation and/or Photodetachment of Atmospheric Negative Ions: Initial Results on O_2^- and CO_3^-." BRL Memorandum Report No. 2594 (USA BRL, Aberdeen Proving Ground, MD, 1976). (AD #A021935)

$\sigma_{A^+}(\lambda_1)$ is the photodissociation cross section for a positive ion (A^+) at a photon wavelength λ_1. $\sigma_{O^-}(\lambda_1)$ is the photodetachment cross section for O^- at the same wavelength.[5] The value for $\sigma_{O^-}(\lambda_1)$ is obtained from the results of Branscomb *et al.*[5] and used for normalization purposes. The ratio of the number of detected A^+ counts for laser off (N_o) and laser on ($N(\lambda_1)$) is given by $(N_o/N(\lambda_1))_{A^+}$. This ratio for detected O^- counts is $(N_o/N(\lambda_1))_{O^-}$. The ratio of the laser powers for the O^- and A^+ measurements are given by $P = P_{O^-}(\lambda_1)/P_{A^+}(\lambda_1)$. The laser power in most cases is held constant and hence does not affect Equation 1. A geometric factor describing the overlap between the ion beam and photon beam is normally required to calculate a photodissociation cross section; however, it has been assumed that this overlap factor remains the same for the measurement of O^- and A^+. Thus this factor does not appear in Equation 1. Values for the ion velocities, v_{A^+} and v_{O^-}, are obtained from published mobilities where possible. If published values are not available a mass scaling procedure is used.[3]

Discrete lines available from argon ion and krypton ion lasers as well as lines from a tunable pumped dye laser have been used for the present experiments. The prism selected photon energies have a resolution of $\sim 10^{-5}$ eV and the dye laser lines a resolution of $\sim 10^{-3}$ eV. With proper otpics a krypton ion laser can be made to lase on at least 13 discrete lines. All lines except four were prism selected; the violet lines, 415.4 and 4.3.1 nm, were made to lase with mirror coatings only, hence both lines lased simultaneously. The same situation applies for the 356.4 and 350.7 nm lines.

Relative and absolute uncertainties are associated with the data reported in this paper. The total relative error is given by the error bars on the various figures. This relative error is composed of statistical counting error, variations in parameters that determine the ion drift velocity (pressure, temperature, and the drift field), and the uncertainty in the relative laser power measurement. The statistical counting error is taken as $\pm\sqrt{N}$ and the root mean square error of the other contributions results in a ± 5% estimate. These two numbers are then combined (root mean square) to give an estimate of the total relative error. In addition to the relative error there exists an absolute error of ± 10%[5] in the photodetachment cross section value for O^-. An absolute error also exists in the reduced mobilities used to compute the ion drift velocities. These errors are ± 5% for O^- in O_2[6] and ± 3%

---

[5] L. M. Branscomb, S. J. Smith, and G. Tisone, "Oxygen Metastable Atom Production Through Photodetachment," J. Chem. Phys. 43, 2906-2907 (1965).

[6] R. M. Snuggs, D. J. Volz, J. H. Schummers, D. W. Martin, and E. W. McDaniel, "Ion Molecule Reactions Between O^- and O_2^- at Thermal Energies and Above," Phys. Rev. 178, 240-248 (1969).

for $NO^+(NO)$ in NO.[7] The mobilities for $NO^+(H_2O)$ in NO and in Ar were obtained by mass scaling and a conservative absolute error of ± 20% was assigned to mobilities obtained in this fashion. The root mean square absolute error for $NO^+(NO)$ is ± 12% and ± 23% for $NO^+(H_2O)$. The total error must be computed point by point.

III. RESULTS

A. $NO^+(NO)$

$NO^+(NO)$ cluster ions were formed in 40.0-46.6 N/m^2 (133.3 N/m^2 = 1 Torr) nitric oxide gas (minimum specified purity of 99.0%) by the following reactions:

$$NO + e \rightarrow NO^+ + 2e \qquad \text{I}$$

and

$$NO^+ + 2NO \leftrightarrow NO^+(NO) + NO. \qquad \text{II}$$

The photodissociation cross section for $NO^+(NO)$ was measured as a function of laser power, E/N, drift distance, pressure, and photon energy. All of these measurements were made at room temperature, ~ 300°K. By normalizing the photodissociation cross section to the known cross section values for the photodetachment cross section of O^- (see Equation 1), the measured cross sections were placed on an absolute scale. The only changes in experimental conditions made between the O^- and $NO^+(NO)$ measurements were reversing appropriate voltages, tuning the electron energy in the source for optimum production of O^-, and replacing the NO gas with an equal pressure of research grade O_2 gas. The ion velocities for O^- in O_2 and $NO^+(NO)$ in NO were obtained from published mobility values.[6,7]

Figure 1 shows the measured photodissociation cross section for $NO^+(NO)$ as a function of laser power for two different photon wavelengths (647.1 and 530.9 nm). The E/N was held constant at 15 x 10^{-17} V - cm^2 and the drift distance from the exit of the source to the sampling aperture was fixed at 7.5 cm. It is readily observed that the cross section is not independent of laser power for either photon wavelength. These two discrete wavelengths are the most intense lines produced from the krypton ion laser and the fraction of $NO^+(NO)$ ions destroyed can be substantial, approaching 80% for the 647.1 nm line at high laser power.

The photodissociation of $NO^+(NO)$ is also observed to be dependent on E/N as can be seen on Figure 2. The photon wavelength was fixed at 530.9 nm and the open circles represent data obtained at approximately half the laser power as that for the open triangles. The photodissociation cross section decreases with decreasing E/N. It can also be observed

---

[7] Volz, D. J., J. H. Schummers, R. D. Laser, D. W. Martin, and E. W. McDaniel, "Mobilities and Longitudinal Diffusion Coefficients of Mass-Identified Potassium Ions and Positive Nitric Oxide Ions in Nitric Oxide," Phys. Rev. A 4, 1106-1109 (1971).

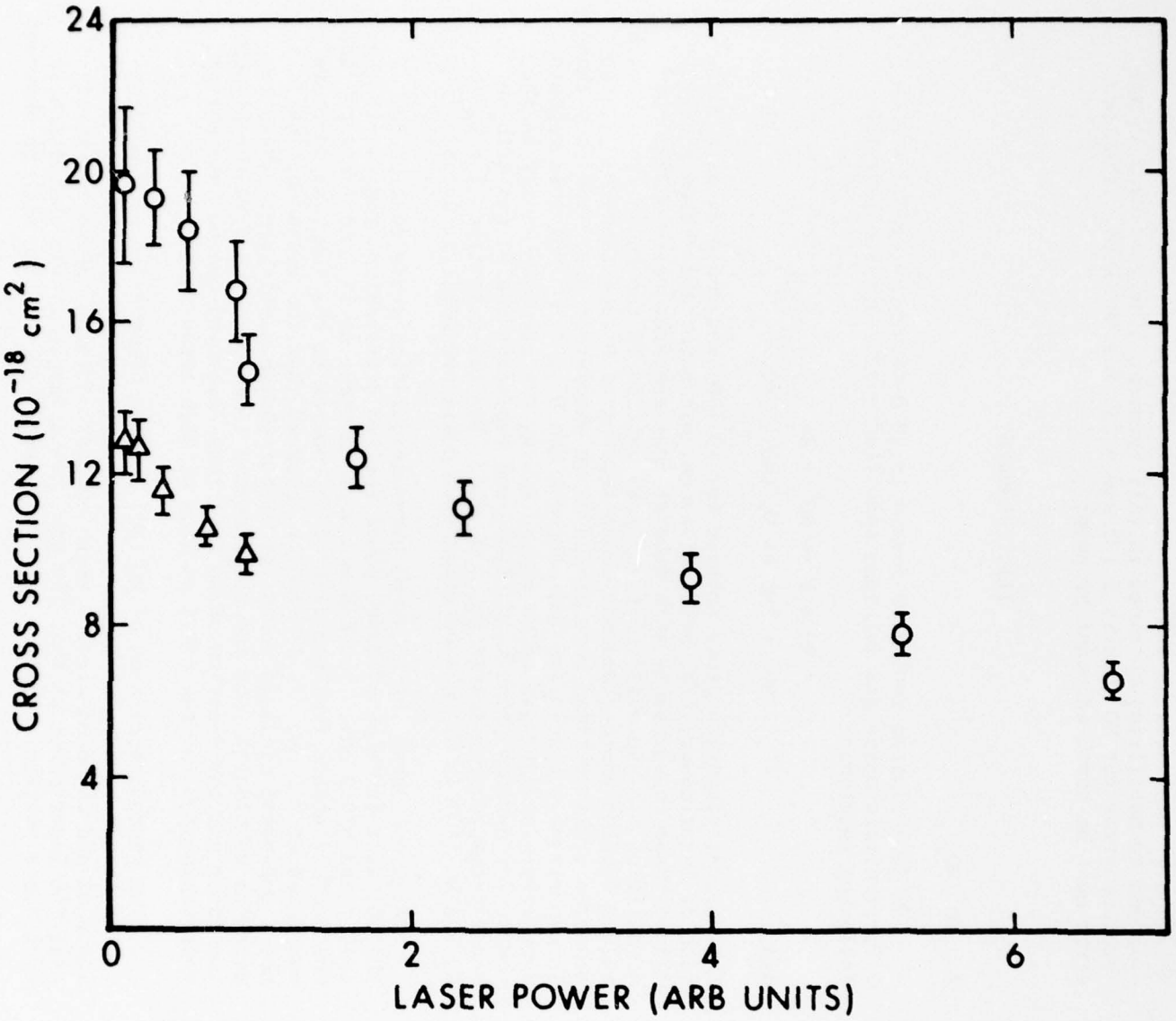

Figure 1. Photodissociation cross section versus laser power for $NO^+(NO)$. The open circles represent a photon wavelength of 647.1 nm and the open triangles are at 530.9 nm.

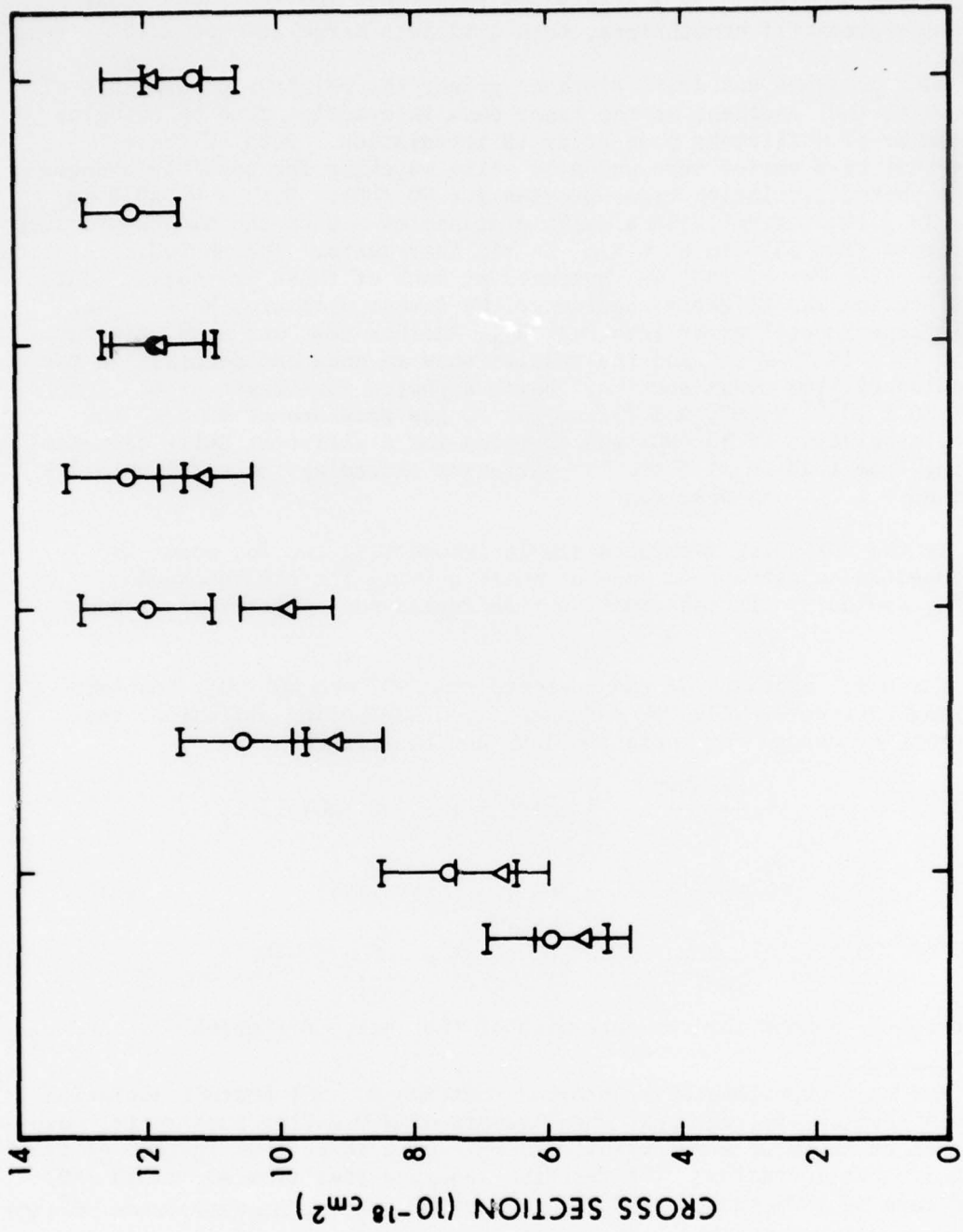

Figure 2. Photodissociation cross section versus E/N for $NO^+(NO)$. The open circles represent data taken at approximately twice the laser power of the open triangle data.

from Fig. 2 that the open triangle values obtained with the higher laser power start decreasing at a higher E/N than those for the lower laser power measurements; nonetheless, both data sets merge at ~ 30 x 10^{-17} V-cm^2.

Both pressure and drift distance affect the relative populations of NO^+ and $NO^+(NO)$ incident at the laser beam interaction zone by changing the number of collisions made prior to irradiation. Both of these parameters were varied independently while watching for possible changes in the photodissociation cross section for $NO^+(NO)$. With λ = 730.0 nm, E/N = 30 x 10^{-17} V-cm^2, and a drift distance of 5.6 cm the NO gas pressure was varied from 33.3 to 66.6 N/m^2 in six increments. The photodissociation cross section for $NO^+(NO)$ was measured at each of these pressures. This cross section was slightly smaller at the lowest pressure, however well within experimental error (see Fig. 3). Another test was made using an E/N of 15 x 10^{-17} V-cm^2 and the results show an enhanced decrease in the photodissociation cross section. Using a photon wavelength of 647.1 nm, E/N = 30 x 10^{-17} V-cm^2, and fixing the NO gas pressure at 40 N/m^2 the photodissociation of $NO^+(NO)$ was observed for 6 different drift distances ranging from 1.88 to 11.3 cm. No variation exceeding the total relative error of ~ ± 15% was observed.

In the following section a simple interacting two ion model is developed in an attempt to account qualitatively for the observed $NO^+(NO)$ photodissociation cross section dependence on laser power and E/N.

The model consists of two positive ions, NO^+ and $NO^+(NO)$, that are drifting together coupled by reaction II.* Neglecting diffusion, the time rate of change for these two ions can be written as

$$\frac{d[NO^+]}{dt} = -\nu_1[NO^+] + \nu_2[NO^+(NO)] \qquad (2)$$

and

$$\frac{d[NO^+(NO)]}{dt} = \nu_1[NO^+] - \nu_2[NO^+(NO)] \qquad (3)$$

where $k_1 = \frac{\nu_1}{[NO]^2}$ and $k_2 = \frac{\nu_2}{[NO]}$.

The brackets denote the concentration of the enclosed species. ν_1 and ν_2

*It has been experimentally observed that the $NO^+(NO)$ photodissociation cross section will decrease when amounts of H_2O giving substantial quantities of $NO^+(H_2O)$ are present. In this case three ions instead of two require consideration. The reaction sequence goes from NO^+ to $NO^+(NO)$ and then $NO^+(NO)$ reacts with H_2O to form $NO^+(H_2O)$. However, when $NO^+(NO)$ is photodissociated the collisional dissociation rate of $NO^+(H_2O)$ can repopulate $NO^+(NO)$ very fast under certain conditions. Here, the photodissociation measurements for $NO^+(NO)$ were made where the $NO^+(H_2O)$ ion was present only in trace quantities.

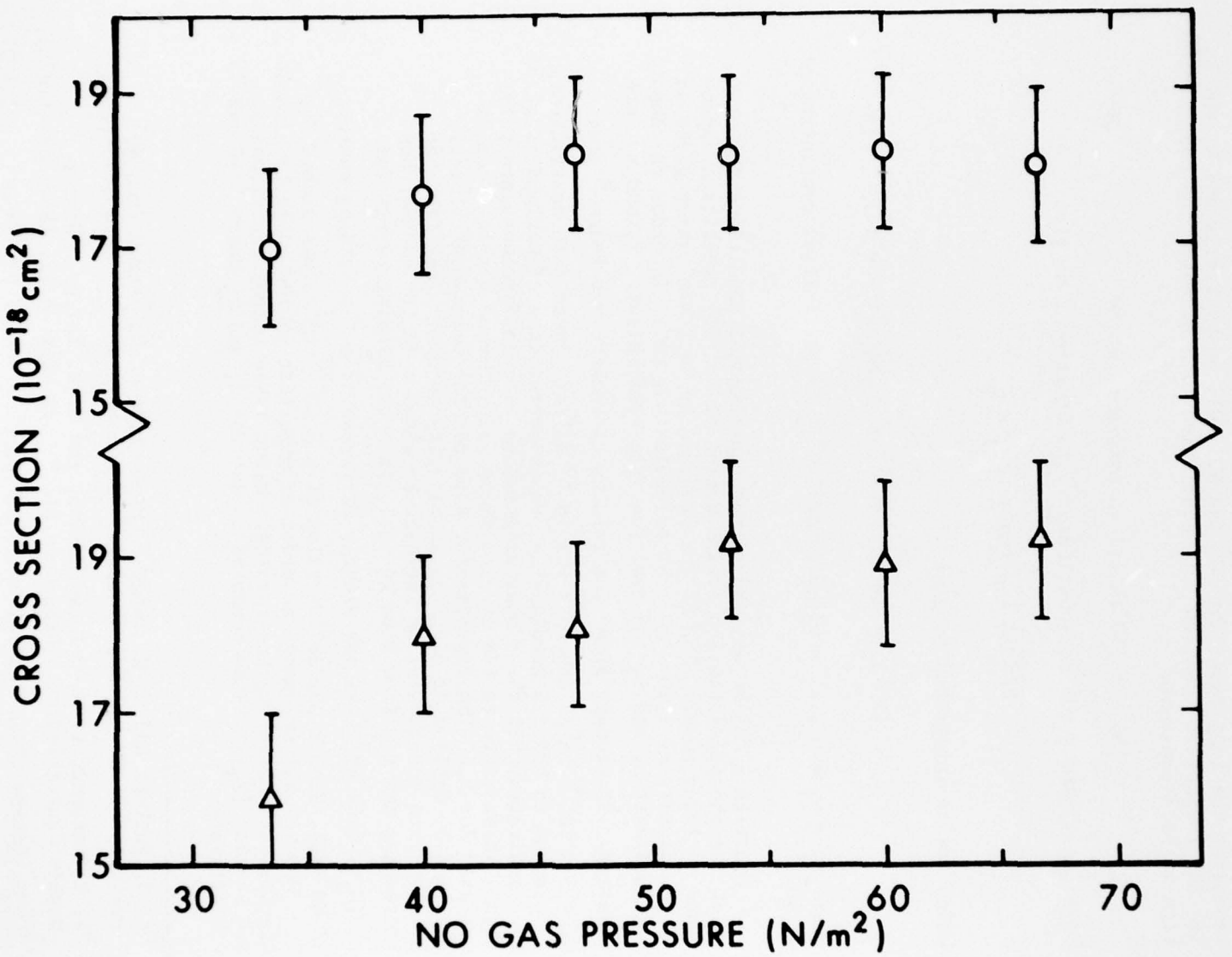

Figure 3. Photodissociation cross section versus NO pressure for $NO^+(NO)$. The open circle data were obtained at an E/N of 30 x 10^{-17} V-cm^2, the open triangles 15 x 10^{-17} V-cm^2.

represent the loss rates for NO^+ and $NO^+(NO)$, respectively and k_1 and k_2 are the respective reaction rate coefficients. The total ion concentration is held constant,

$$[NO^+] + [NO^+(NO)] = \text{constant} = [N_T] \qquad (4)$$

Equations 3 and 4 can be substituted into Equation 2 to give

$$\frac{d[NO^+]}{dt} + c_1[NO^+] - c_2 = 0,$$

which can be integrated to give

$$[NO^+]_t = [NO^+]_o \; e^{-c_1 t} + (c_2/c_1)(1 - e^{c_1 t}) \qquad (5)$$

where $c_1 = \nu_1 + \nu_2$, $c_2 = \nu_2[N_T]$, and $[NO^+]_o$ is the initial concentration of NO^+.

Equation 5 can be applied to the experimental conditions for which the photodissociation cross section of $NO^+(NO)$ exhibits a dependence on laser power. The NO gas pressure is 46.5 N/m^2 which gives an NO gas density of 1.13×10^{16} NO molecules per cm^3. In order to compute the constants c_1 and c_2 the reaction rate coefficients, k_1 and k_2, are required. Stationary afterglow results of Puckett and Teague[8] give $k_1 = 5 \times 10^{-30}$ cm^6/s and $k_2 = 9 \times 10^{-16}$ cm^3/s. These rate coefficients correspond to $E/N \sim 0$ conditions. Experimental data of Gatland *et al.*[9] have indicated that three body association rate coefficients are relatively insensitive to E/N for low field values; hence 5×10^{-30} cm^6/s was used for k_1. The experimental data for the breakup of $Li^+(N_2)$ obtained by Gatland *et al.* show sensitivity to E/N. They find the breakup rate coefficient to increase by about a factor of two when increasing the E/N from 9 to 24 Td. Since the binding energy for $Li^+(N_2)$, 0.54 eV,[10] is not greatly different from the binding energy of $NO^+(NO)$, $0.63 \pm .09$ eV[11] a value of 2×10^{-15} cm^3/s was picked for k_2. However k_2 can change an order of magnitude in the analysis without significantly altering the results. Using these values for k_1 and k_2 and setting $[N_T] = 1$ the computed values for c_1 and c_2 become 640 and 23 s^{-1}, respectively.

---

[8] L. J. Puckett and M. W. Teague, "Production of $H_3O^+ \cdot nH_2O$ from NO^+ Precursor in NO-H_2O Gas Mixtures," J. Chem. Phys. 54, 2564-2572 (1971).

[9] I. R. Gatland, L. M. Colonna-Romano, and G. E. Keller, "Single and Double Clustering of Nitrogen to Li^+," Phys. Rev. A 12, 1885-1894 (1975).

[10] K. G. Spears, "Ion-Neutral Bonding," J. Chem. Phys. 57, 1850-1858 (1972).

The time frame of interest can be approximated by the time it takes for an ion to traverse the laser beam. The laser beam diameter is approximately 0.3 cm and the ion velocity ranges from 0.3 to 1.9 x 10^4 cm/s, depending on E/N, which gives a time frame of 1.5 to 12.5 x 10^{-5} s. For this time frame Equation 5 reduces effectively to

$$[NO^+]_t = [NO^+]_o e^{-c_1 t}$$

or

$$[NO^+(NO)]_t = 1 - [NO^+]_o e^{-c_1 t}$$

Since $c_1 t << 1$, $[NO^+(NO)]_t \approx 1 - [NO^+]_o + [NO^+]_o c_1 t$. (6)

Typical conditions in the vicinity of the sampling aperture for "laser off" are $[NO^+] = 0.5$ and $[NO^+(NO)] = 0.5$. During "laser on" conditions the apparent fraction of $NO^+(NO)$ ions photodissociated has been experimentally observed to increase from about 10 to 80% by increasing laser power (λ = 647.1 nm). Thus the concentrations of NO^+ can range from 0.55 to 0.90 while that of $NO^+(NO)$ ranges from 0.45 to 0.10. The model can be used to determine the relative extent to which reactions repopulate the $NO^+(NO)$ ion for the two extremes of photodissociation fraction. Using both 0.10 and 0.45 as initial conditions, values for $NO^+(NO)$ as a function of time are computed from Equation 6 and plotted on Figure 4. It can readily be seen from Figure 4 that the larger photodissociation fraction of $NO^+(NO)$ results in a greater deviation of $[NO^+(NO)]_t$ from that of $[NO^+(NO)]_o$. This in turn results in a smaller value for the photodissociation cross section. The model thus predicts that the apparent photodissociation cross section for $NO^+(NO)$ can decrease with increasing laser power in agreement with experimental data.

The sampling time which shall be defined as the time it takes an $NO^+(NO)$ ion to traverse a laser beam diameter is inversely proportional to E/N. E/N values corresponding to different sampling times are designated on the upper abscissa of Figure 4. The plot of $[NO^+(NO)]_t$ as a function of E/N shows that the model also predicts the correct dependence for the photodissociation cross sections with E/N.

Predictions of pressure and drift distance dependences are more complicated and require a detailed knowledge of ion concentrations. Since this model neglects the actual laser beam intensity profile as well as diffusion, further extension of the model was felt unjustified. The photodissociation cross section was experimentally observed to decrease slightly at low pressures and this effect was more apparent at the lower E/N value. These trends are consistent with diffusion effects that might occur in the laser beam interaction zone, nonetheless, at an E/N of 30 x 10^{-17} V-cm^2 the pressure dependence of the photodissociation cross section is well within errors.

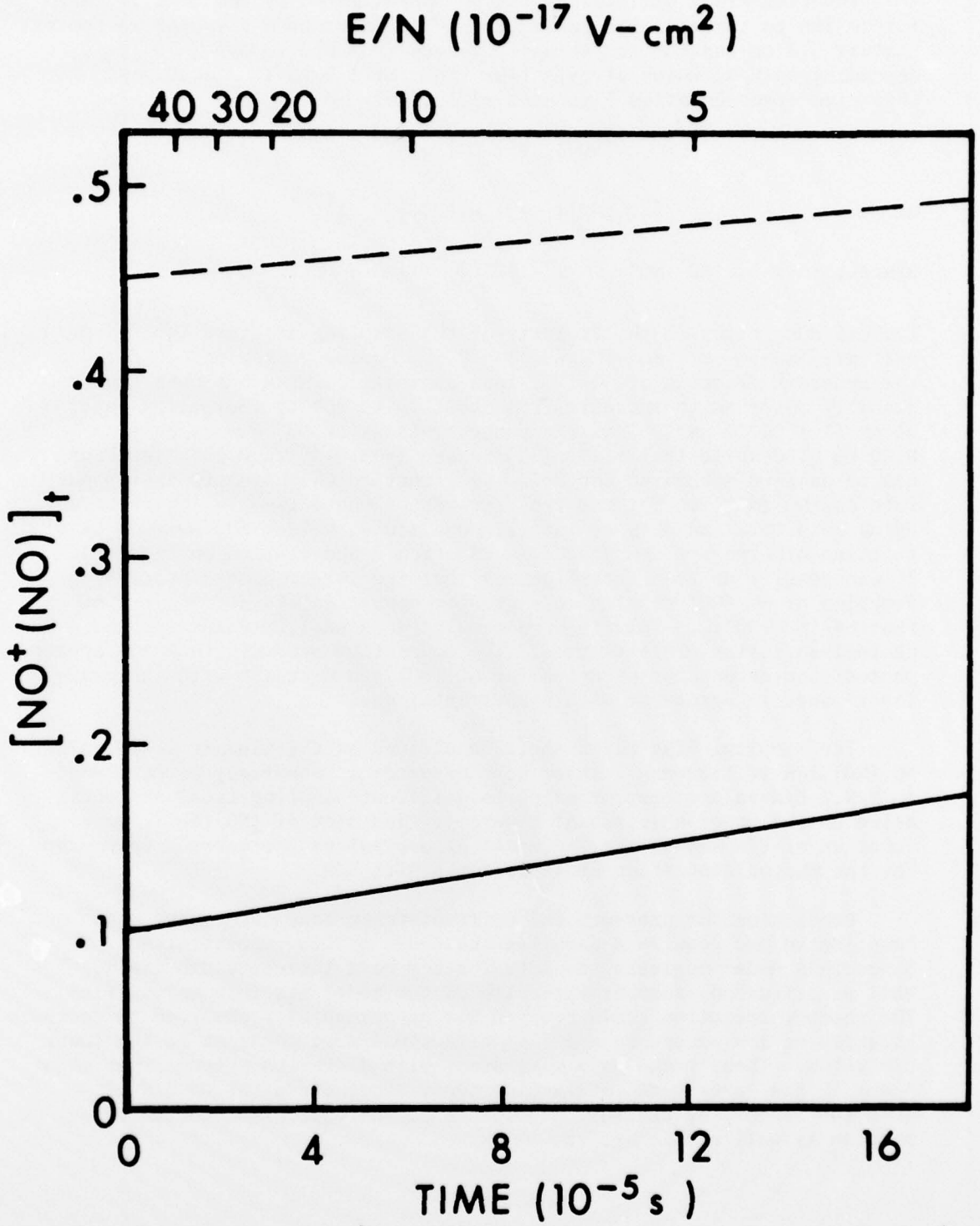

Figure 4. Concentration of $NO^+(NO)$ versus time and E/N for conditions when $NO^+(NO)$ has been greatly perturbed by the laser beam. The solid line represents the case where 80% of the $NO^+(NO)$ ions have been initially photodissociated. The dashed line is for 10% initial photodissociation of $NO^+(NO)$.

The generated model illustrates that there can be a substantial coupling between the photodissociation process and clustering reactions. This model taken along with the experimental data suggests that this coupling can be minimized at low laser power and high E/N, since the perturbation on the ion concentrations of NO^+ and $NO^+(NO)$ increases with increasing laser power or decreasing E/N. Under experimental conditions of low laser power (less than 10% of the $NO^+(NO)$ ions photodissociated), NO pressure of 46.5 N/m^2, and E/N of 30 x 10^{-17} $V\text{-}cm^2$ photodissociation cross sections for $NO^+(NO)$ at other photon wavelengths were measured. These photodissociation cross sections are displayed on Figure 5. The photon energy range covered extends 1.5 to 3.5 eV over which the photodissociation cross section peaks to a value of 1.95 x 10^{-17} cm^2 at about 1.96 eV. Although the cross sections were measured at discrete wavelengths they appear to vary smoothly with wavelength. With the bond energy of $NO^+(NO)$ being 0.63 eV[11] the reaction

$$NO^+(NO) + h\nu \rightarrow NO^+ + NO \qquad \text{III}$$

is highly exothermic for the photon energies used in this experiment. Furthermore no other photodissociation process is energetically possible. An increase in the NO^+ ion during laser-on conditions observed at several photon energies suggests the occurrence of Reaction III. As the photodissociation cross section for $NO^+(NO)$ appears unstructured the photodissociation process is probably occurring between thermal $NO^+(NO)$ and one or more repulsive states of this cluster ion analogous to the photodissociation observed for other "homonuclear" ions, Ar_2^+, Kr_2^+, Xe_2^+[12] and $O_2^+(O_2)$.[3]

B. $NO^+(H_2O)$

Cluster ions of $NO^+(H_2O)$ were produced in 46.5 N/m^2 of NO gas with a trace of H_2O added (< 6.6 x 10^{-3} N/m^2). The dominant reaction path proceeded via Reactions I and II followed by

$$NO^+(NO) + H_2O \rightarrow NO^+(H_2O) + NO \qquad \text{IV}$$

Measurements for the photodissociation cross section of $NO^+(H_2O)$ produced by this method were obtained by again using O^- for normalization and the drift velocity of $NO^+(H_2O)$ in NO was calculated by mass scaling to the value of K^+ drifting in NO gas. The reduced mobility computed in this manner was 2.15 $cm^2/V\text{-}s$. The measured cross section for the photodissociation of $NO^+(H_2O)$ was found to be dependent on drift distance as

---

[11] D. B. Dunkin, F. C. Fehsenfeld, A. L. Schmeltekopf, and E. E. Ferguson, "Three Body Association Reactions of NO^+ with O_2, N_2, and CO_2," J. Chem. Phys. 54, 3817-3822 (1971).

[12] T. M. Miller, J. H. Ling, and J. T. Moseley, "Absolute Total Cross Sections for the Photodissociation of Ar_2^+, Kr_2^+, Xe_2^+, ArN_2^+, KrN_2^+, and KrN^+ from 565 to 695 nm," Phys Rev. A 13, 2171-2177 (1976).

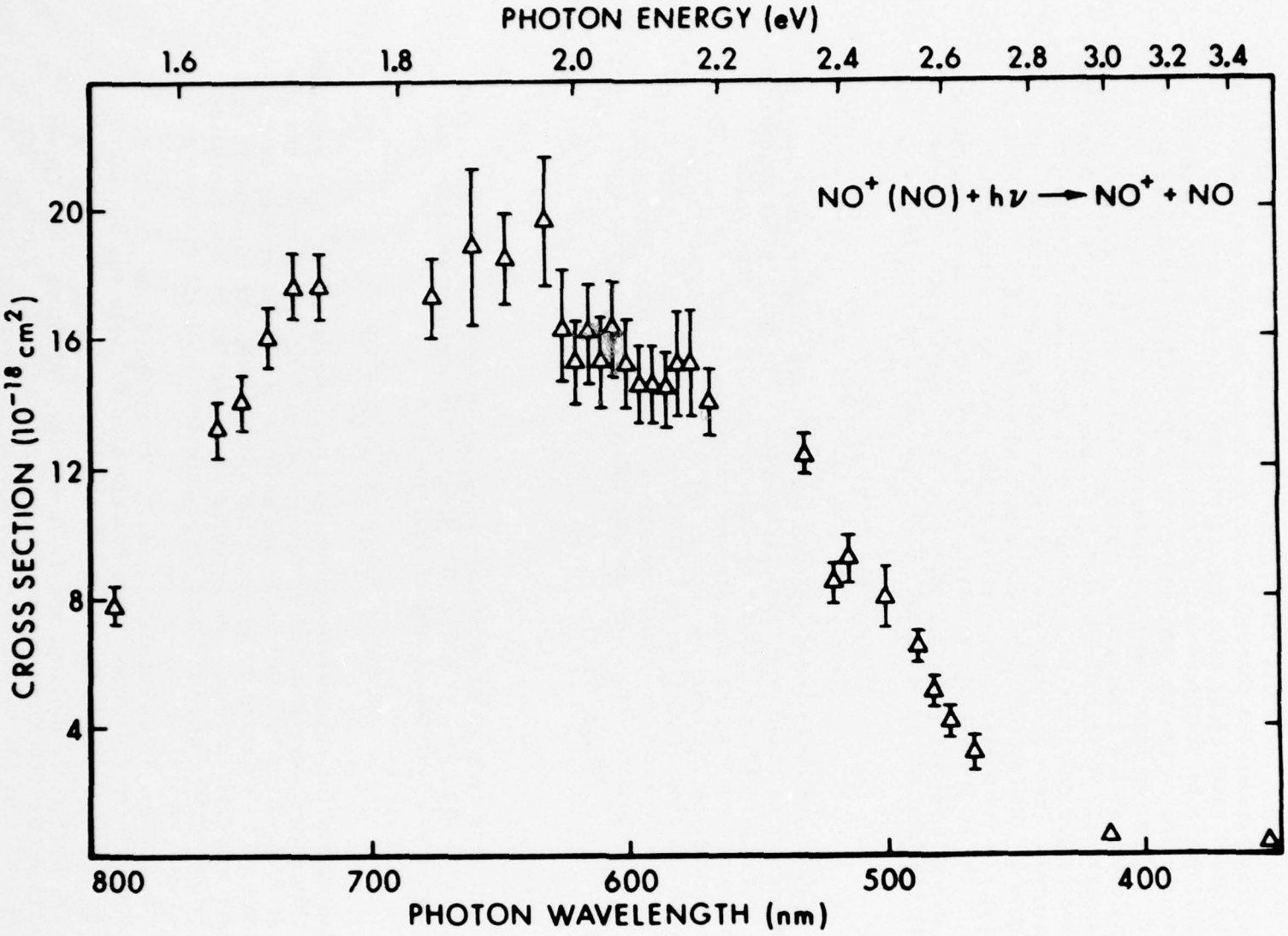

Figure 5. Photodissociation cross section versus photon wavelength for $NO^+(NO)$.

is shown on Figure 6. The open triangles represent data taken at 647.1 nm and the open circles data taken at 530.9 nm. The E/N was held fixed at 30×10^{-17} V-cm^2. A decrease in cross section with increasing drift distance is observed and the rate of decrease appears to be the same for both photon wavelengths.

Vibrational excitation of the $NO^+(H_2O)$ cluster ion might account for this behavior if some vibrationally excited state or states which can be photodissociated are relaxing as a function of drift distance. However, it is not clear why this dependence should be so similar for two substantially different photon wavelengths.

Further investigations of the drift distance behavior were conducted by creating the $NO^+(H_2O)$ cluster ions in a buffer gas of argon (19.9 N/m^2 Ar, .66 N/m^2 NO, and ~ .66 N/m^2 H_2O). In this case the dominant reaction path is Reactions I and II along with

$$Ar + e \rightarrow Ar^+ + 2e, \qquad V$$

$$Ar^+ + NO \rightarrow NO^+ + Ar \qquad VI$$

and

$$NO^+ + H_2O + Ar \rightarrow NO^+(H_2O) + Ar. \qquad VII$$

Photodissociation measurements of $NO^+(H_2O)$ produced by this method indicated that the cross section was small or zero at 647.1 nm for all drift distances.

An explanation for this difference in the $NO^+(H_2O)$ photodissociation cross sections is necessary before either set of measurements can be considered as valid. One principal difference in the two methods of producing $NO^+(H_2O)$ is that in one case $NO^+(NO)$ is formed prior to the formation of $NO^+(H_2O)$. Since $NO^+(NO)$ has a large photodissociation cross section at 647.1 nm this cluster ion is substantially depleted during "laser on" conditions. This effect causes Reaction IV to be inhibited in the ion swarm volume intersected by the laser beam. $NO^+(H_2O)$ is being formed throughout the drift distance; therefore inhibiting Reaction IV will result in a decrease of the $NO^+(H_2O)$ signal irrespective of possible photodissociation of the ion.

This effect can also qualitatively explain the drift distance dependence. The fractional decrease in the $NO^+(H_2O)$ signal should be proportional to the laser beam diameter divided by the total formation distance for $NO^+(H_2O)$. As the drift distance increases, this ratio becomes smaller. A plot of this ratio versus the drift distance is shown on Figure 6 as the solid line. Since the ion source is of finite length, estimated as ~ 2 cm, this distance was added to the drift distance in computing the total formation distance for $NO^+(H_2O)$. The shape

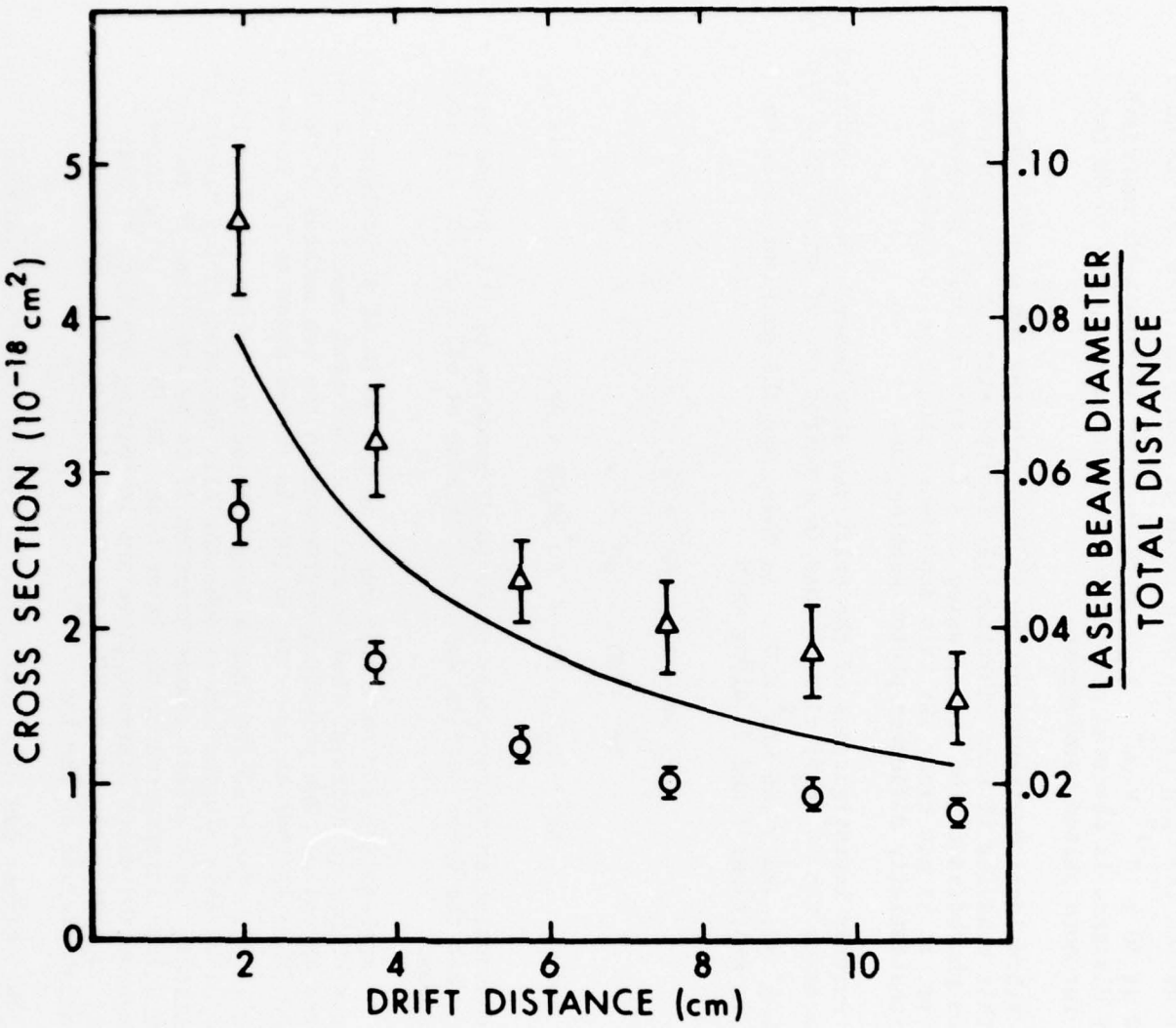

Figure 6. Apparent photodissociation cross section versus drift distance for $NO^+(H_2O)$; also the ratio of the laser beam diameter to the total drift distance versus drift distance for $NO^+(H_2O)$. The open circles represent data taken at 530.9 nm, the open triangles 647.1 nm. The solid line represents a plot of the ratio of the laser beam diameter to total distance versus drift distance for the conditions of the experiment.

of this solid line tracks extremely well with the photodissociation cross section dependence on drift distance and thus adds validity to the mechanism proposed.

When the argon buffer is used to create $NO^+(H_2O)$ the intermediate ion $NO^+(NO)$ is no longer in the dominant reaction path and hence the measurements made in this way are believed to reflect the actual photodissociation cross section values. No actual photodissociation was observed for $NO^+(H_2O)$ at the various photon energies studied. Upper limits for the photodissociation cross sections for $NO^+(H_2O)$ were computed and are listed in Table I.

TABLE 1. UPPER LIMITS FOR THE PHOTODISSOCIATION CROSS SECTIONS OF $NO^+(H_2O)$.

Photon Energy (eV)	Cross Section (10^{-18} cm^2)
1.5510	0.1
1.6474	0.1
1.9158	0.05
2.032	0.1
2.175	0.3
3.0	0.15
3.5	0.15

IV. SUMMARY

Two atmospheric ions $NO^+(NO)$ and $NO^+(H_2O)$ have been investigated for possible photodissociation reactions. $NO^+(NO)$ was observed to readily photodissociate while the photodissociation cross section for $NO^+(H_2O)$ was small or zero for the photon energies studied.

A simple model has been used to explain the observed behavior of the $NO^+(NO)$ photodissociation cross section with respect to laser power and E/N. In the studies of $NO^+(H_2O)$ a mechanism that can result in an "apparent" photodissociation cross section was observed. Measurement of the photodissociation of an ion formed through an intermediate ion of large photodissociation cross section can be misleading because of the inhibition of reactions linking the two ions.

ACKNOWLEDGMENT

I express thanks to Dr. M. S. Miller for many helpful discussions on the contents of this manuscript.

REFERENCES

1. E. E. Ferguson, "D-Region Ion Chemistry," Rev. Geophys. and Space Phys. 9, 997-1007 (1971).

2. J. A. Vanderhoff and R. A. Beyer, "Photodissociation of $O_2^+(H_2O)$," Chem. Phys. Lett. 38, 532-536 (1976).

3. R. A. Beyer and J. A. Vanderhoff, "Cross Section Measurements for Photodetachment or Photodissociation of Ions Produced in Gaseous Mixtures of O_2, CO_2, and H_2O," J. Chem. Phys. 65, 2313-2321 (1976).

4. J. A. Vanderhoff and R. A. Beyer, "Experimental Photodissociation and/or Photodetachment of Atmospheric Negative Ions: Initial Results on O_2^- and CO_3^-." BRL Memorandum Report No. 2594 (USA BRL, Aberdeen Proving Ground, MD, 1976).

5. L. M. Branscomb, S. J. Smith, and G. Tisone, "Oxygen Metastable Atom Production Through Photodetachment," J. Chem. Phys. 43, 2906-2907 (1965).

6. R. M. Snuggs, D. J. Volz, J. H. Schummers, D. W. Martin, and E. W. McDaniel, "Ion Molecule Reactions Between O^- and O_2^- at Thermal Energies and Above," Phys. Rev. 178, 240-248 (1969).

7. Volz, D. J., J. H. Schummers, R. D. Laser, D. W. Martin, and E. W. McDaniel, "Mobilities and Longitudinal Diffusion Coefficients of Mass-Identified Potassium Ions and Positive Nitric Oxide Ions in Nitric Oxide," Phys. Rev. A 4, 1106-1109 (1971).

8. L. J. Puckett and M. W. Teague, "Production of $H_3O^+ \cdot nH_2O$ from NO^+ Precursor in NO-H_2O Gas Mixtures," J. Chem. Phys. 54, 2564-2572 (1971).

9. I. R. Gatland, L. M. Colonna-Romano, and G. E. Keller, "Single and Double Clustering of Nitrogen to Li^+," Phys. Rev. A 12, 1885-1894 (1975).

10. K. G. Spears, "Ion-Neutral Bonding," J. Chem. Phys. 57, 1850-1858 (1972).

11. D. B. Dunkin, F. C. Fehsenfeld, A. L. Schmeltekopf, and E. E. Ferguson, "Three Body Association Reactions of NO^+ with O_2, N_2, and CO_2," J. Chem. Phys. 54, 3817-3822 (1971).

12. T. M. Miller, J. H. Ling, and J. T. Moseley, "Absolute Total Cross Sections for the Photodissociation of Ar_2^+, Kr_2^+, Xe_2^+, ArN_2^+, KrN_2^+, and KrN^+ from 565 to 695 nm," Phys Rev. A 13, 2171-2177 (1976).

DISTRIBUTION LIST

No. of Copies	Organization
12	Commander Defense Documentation Center ATTN: DDC-TCA Cameron Station Alexandria, VA 22314
1	Director Institute for Defense Analyses ATTN: Dr. E. Bauer 400 Army-Navy Drive Arlington, VA 22202
2	Director Defense Advanced Research Projects Agency ATTN: STO, CPT J. Justice Dr. S. Zakanyca 1400 Wilson Boulevard Arlington, VA 22209
1	Director of Defense Research & Engineering ATTN: CAPT K. W. Ruggles Washington, DC 20305
4	Director Defense Nuclear Agency ATTN: STAP (APTL) STRA (RAAE), Dr. C. Blank Dr. H. Fitz, Jr. DDST Washington, DC 20305
2	DASIAC/DOD Nuclear Information & Analysis Center General Electric Company-TEMPO ATTN: Mr. A. Feryok Mr. W. Knapp 816 State Street P.O. Drawer QQ Santa Barbara, CA 93102
1	Director Defense Communications Agency ATTN: Code 340, Mr. W. Dix Washington, DC 20305
1	Commander US Army Materiel Development and Readiness Command ATTN: DRCDMA-ST 5001 Eisenhower Avenue Alexandria, VA 22333
1	Commander US Army Aviation Research & Development Command ATTN: DRSAV-E 12th and Spruce Streets St. Louis, MO 63166
1	Director US Army Air Mobility Research and Development Laboratory Ames Research Center Moffett Field, CA 94035
1	Commander US Army Electronics Command ATTN: DRSEL-RD Fort Monmouth, NJ 07703
5	Commander/Director Atmospheric Sciences Laboratory US Army Electronics Command ATTN: Dr. E. H. Holt Mr. H. Ballard Dr. F. E. Niles Dr. M. G. Heaps Dr. D. E. Snider White Sands Missile Range, NM 88002
1	Commander US Army Missile Research and Development Command ATTN: DRDMI-R Redstone Arsenal, AL 35809

DISTRIBUTION LIST

No. of Copies	Organization
1	Commander US Army Tank-Automotive Development Command ATTN: DRDTA-RWL Warren, MI 48090
2	Commander US Army Mobility Equipment Research & Development Command ATTN: Tech Docu Cen, Bldg 315 DRSME-RZT Fort Belvoir, VA 22060
1	Commander US Army Armament Research & Development Command Dover, NJ 07801
2	Commander US Army Harry Diamond Laboratories ATTN: DRXDO-TI DRXDO-NP, Mr. F. Wimenitz 2800 Powder Mill Road Adelphi, Maryland 20783
1	Director US Army TRADOC Systems Analysis Agency ATTN: ATAA-SA White Sands Missile Range, NM 88002
1	Commander US Army Nuclear Agency ATTN: Mr. J. Berberet Fort Bliss, Texas 79916
1	Commander US Army Research Office ATTN: Dr. R. Lontz P.O. Box 12211 Research Triangle Park NC 27709
1	HQDA (DAEN-RDM/Dr. de Percin) WASH DC 20314
1	Chief of Naval Research ATTN: Code 418, Dr. J. Dardis Department of the Navy Washington, DC 20360
1	Commander US Naval Electronics Laboratory ATTN: Mr. W. Moler San Diego, CA 92152
1	Commander US Naval Surface Weapons Center ATTN: Dr. L. Rutland Silver Spring, MD 20910
3	Commander US Naval Research Laboratory ATTN: Dr. W. Ali Code 7700, Mr. J. Brown Code 2020, Tech Lib Washington, DC 20375
3	HQ USAF (AFNIN; AFRD; AFRDQ) Washington, DC 20330
7	AFGL (LKD, Dr. R. Narcisi, LKB, Dr. K. Champion, Dr. T. Keneshea, Dr. J. Paulson Dr. W. Swider OPR, Dr. Murphey Dr. Kennelly Hanscom AFB, MA 01730
2	AFSC (DLCAW, LTC R. Linkous; SCS) Andrews AFB Washington, DC 20334
1	Director National Oceanic and Atmospheric Administration ATTN: Dr. E. Ferguson US Department of Commerce Boulder, CO 80302

DISTRIBUTION LIST

No. of Copies	Organization
1	Director Brookhaven National Laboratory ATTN: Docu Sec 25 Brookhaven Avenue Upton, NY 11973
1	Director Jet Propulsion Laboratory ATTN: Dr. W. Huntress 4800 Oak Grove Drive Pasadena, CA 91103
2	Director Los Alamos Scientific Laboratory ATTN: Lib Dr. W. Maier (Gp J-10) P.O. Box 1663 Los Alamos, NM 87544
2	Sandia Laboratories ATTN: Org 3141, Tech Lib Org 100, F. Hudson P.O. Box 5800 Albuquerque, NM 87115
1	Bell Telephone Laboratories, Inc. Technical Report Service ATTN: Tech Rpts Specialist Whippany, NJ 07981
1	General Electric Company Valley Forge Space Technology Center ATTN: Dr. M. Bortner P.O. Box 8555 Philadelphia, PA 19101
1	Mission Research Corporation ATTN: Dr. M. Scheibe 735 State Street P.O. Drawer 719 Santa Barbara, CA 93102
1	R&D Associates ATTN: Dr. F. Gilmore P.O. Box 9695 Marina del Rey, CA 90291
4	Stanford Research Institute ATTN: Dr. J. Peterson Dr. J. Moseley Dr. P. Cosby Dr. F. Smith 333 Ravenswood Avenue Menlo Park, CA 94025
1	CIRES University of Colorado ATTN: Dr. A. W. Castleman Boulder, CO 80302
1	Georgia Institute of Technology School of Physics ATTN: I. R. Gatland Atlanta, GA 30332
1	Pennsylvania State University Ionospheric Research Laboratory ATTN: Dr. L. C. Hale University Park, PA 16802
1	State University of New York Department of Atmospheric Sciences ATTN: Dr. V. Mohnen Albany, NY 12203
2	University of Colorado Joint Institute for Laboratory Astrophysics ATTN: Dr. W. C. Lineberger Dr. A. V. Phelps Boulder, CO 80304
1	University of Delaware Department of Physics ATTN: Prof. S. B. Woo Newark, DE 19711

DISTRIBUTION LIST

No. of Copies	Organization
1	University of Denver Denver Research Institute ATTN: Dr. R. Amme P.O. Box 10127 Denver, CO 82010
1	University of Illinois Electrical Engineering Department Aeronomy Laboratory ATTN: Prof. C. Sechrist Urbana, IL 61801
1	University of Minnesota, Morris Division of Science and Mathematics ATTN: Dr. M. N. Hirsh Morris, MN 56267
1	University of Missouri-Rolla Department of Physics ATTN: Dr. R. Anderson 105 Physics Bldg. Rolla, MO 65401
1	University of Pittsburgh Cathedral of Learning ATTN: Dr. M. A. Biondi 400 Bellefield Avenue Pittsburgh, PA 15213
1	University of Texas at El Paso Physics Department ATTN: J. Collins El Paso, TX
1	University of Utah Chemistry Department ATTN: Dr. M. L. Vestal Salt Lake City, UT 84112
	Aberdeen Proving Ground
	Marine Corps LnO Dir, USAMSAA